Glued-in rods in cross laminated timber – Numerical simulations and parametric studies

Boris Azinović [a,*], Henrik Danielsson [b], Erik Serrano [b], Miha Kramar [a]

[a] *Section for Timber Structures, Slovenian National Building and Civil Engineering Institute (ZAG), Ljubljana, Slovenia*
[b] *Division of Structural Mechanics, Lund University, Sweden*

HIGHLIGHTS

- Glued-in rod connections have high potential for use in CLT structures.
- FE analyses of various connections with glued-in rods in CLT performed.
- Different rod diameters, glued-in lengths and rod-to-grain angles studied.
- Capacity of the connection increases with the glued-in length and the rod diameter.
- Connections with rod perpendicular to grain have higher load bearing capacities.

ARTICLE INFO

ABSTRACT

Numerical simulations and parametric studies of glued-in rods in cross-laminated timber have been performed. The simulations were based on 3D finite element analysis, using a cohesive surface model for the bond-lines between the laminations and the bond-line along the rod. The parametric studies investigated the influence of the glued-in length, the rod diameter, and the rod-to-grain angle on the load-bearing capacity and stiffness of the connection. The analyses showed that the load-bearing capacity generally increases with the glued-in length and the rod diameter, which agrees well with experiments. For different rod-to-grain angles, different mechanical behaviour was observed, especially considering the failure modes.

1. Introduction

Glued-in rods in timber elements are considered to be a highly efficient type of connection, mainly for the following reasons: (i) higher strength and stiffness compared to dowel-type fasteners, (ii) good fire resistance, (iii) adaptability from the architectural point of view, (iv) relatively low overall cost, and (v) the possibility of production in a controlled environment. Glued-in rods have been used in practice for many years, extensively for glued laminated timber and to some extent also for laminated veneer lumber (LVL) applications. Experimental research dates back to the 1980's, e.g. the work of Riberholt [1], Kangas [2] and Ehlbeck & Siebert [3].

As regards cross laminated timber (CLT), experience is very limited, although it is probable that glued-in rods could be used efficiently also in the case of CLT. Different applications in CLT are possible, such as: (i) connections between CLT walls, (ii) connections between CLT walls and beams, (iii) connections between CLT and structural elements made of other materials (e.g., CLT-steel and CLT-concrete). Due to the increased interest in the construction of mid- to high-rise structures with CLT, there is a need for research covering the mechanical resistance of glued-in rod connections for CLT.

One of very few reports on the behaviour of glued-in rods in the case of CLT can be found in [4], where the results of a combined experimental and numerical study are presented. The failure modes and pull-out strengths of 12 different specimen types were studied. All the specimens were bonded with epoxy adhesive, and a pull-pull test configuration was used, in which the rod was located in the plane of the CLT. It was found that both the

rod-to-grain angle (i.e. the angle between the longitudinal axis of the rod and the grain direction of the wood in the CLT layer within which the rod is placed) and the composition of the CLT element had an influence on the failure modes, whereas the rod diameter and its glued-in length had an influence on the pull-out load-bearing capacity. It was also concluded that the axial stiffness of the CLT cross section affects the shear stress distribution along the adhesive-timber interface, and so has a significant influence on the pull-out response. The performed study had, however, its limitations in the number of specimens and in the number of variants tested (all the tested rods had a diameter of 12 mm and their maximum glued-in length was 160 mm, whereas two different CLT cross section lay-ups were used, and two different rod-to-grain angles were investigated). This means that the findings of the study cannot be generalised. In another study [5], glued-in rods were used as a part of an innovative connection between a CLT panel and a glulam frame. A polyurethane (PUR) adhesive and different rod-to-grain angles were tested with a pull-compression test configuration. Although neither the glued-in length nor the rod diameter were varied, it was confirmed that the rod-to-grain angle has a strong effect on the pull-out load-bearing capacity, resulting in an increased capacity when the angle is increased. A similar effect was found in the case of the connection's stiffness, which showed a decreasing trend as the rod-to-grain angle was increased.

Apart from the information obtained in the above-mentioned studies [4,5], few reports are available in the literature about the behaviour of glued-in rods in CLT, especially concerning numerical modelling. However, for the purpose of this paper the findings of previous studies related to the modelling of glued-in rods in other materials (e.g. structural timber, glulam and LVL) could, to some extent, be relevant. Several authors have used numerical methods, mostly in form of finite element (FE) analysis, to study the stress distribution in glued-in rod connections. Early examples of the use of FE-analysis in the modelling of glued-in rods can be found in [6–10]. In these studies linear elastic models were applied in order to investigate the stress distribution in the timber-adhesive bond-line, and its dependence on geometrical parameters. A first attempt to use more complex models was presented in 1995 by Johansson et al. [10]. In this study both analytical expressions based on the so-called generalised Volkersen theory, and approaches based on nonlinear FE-analysis including strain-softening behaviour, were included. Later, somewhat more complex modelling approaches were presented by Serrano et al. [11,12], where nonlinear 3D FE-analyses were used to perform theoretical parametric studies, providing an insight into the most influential parameters; e.g. glued-in length, bond-line strength, fracture energy and mode of loading (pull-pull vs. pull-compression). A strain-softening crack band model (similar to a Cohesive Zone Model (CZM)) was used to characterise the behaviour of the adhesive layer between the rod and the timber, whereas a number of analytical expressions based on fracture mechanics were also discussed. The theoretical results were compared to experimental results, showing a good fit [12]. Del Senno et al. [13] established a linear elastic FE-model in order to determine which parameters had the greatest effect on the shear stress distribution in the bond-line. One of their conclusions was that the edge-hole distance has only a small effect on the shear stress distribution. They also found that the shear stress peaks are reduced when the thickness of the glue line is increased, whereas this thickness appears to have a negligible effect on the radial stresses (i.e. on the stresses acting perpendicular to the grain if the rod is placed parallel to the latter). Gardelle and Morlier [14] compared the experimental results with strength predictions which were based on linear elastic FE-analysis, and on analytical nonlinear fracture

mechanics models, using the same approach as Serrano et al. [11,12], showing again that these predictions provide a lower and an upper limit for the failure of glued-in rod connections.

FE-analysis has also been used in some recent studies dealing with glued-in rods or other related fields of timber engineering, such as nailed and screwed timber joints, hold-down connections, and different types of composite timber connections [15–22]. Some of these studies made use of linear elastic 3D FE-analysis in order to investigate the stress response in the connections, whereas others used more elaborate models, including probabilistic models and CZMs to analyse, for instance, the effect of different rod spacings, as well as that of glue-line thickness, on the pull-out load-bearing capacity.

An extensive experimental study of the behaviour of glued-in rods in CLT was recently performed by some of the authors of this paper [23]. The aim of that study was to investigate the differences in response between glued-in rods in CLT and glued-in rods in other materials (e.g. structural timber, glulam, and LVL). For the purposes of the study more than 60 pull-pull tests were performed. The specimens varied in terms of their glued-in length (from 80 to 400 mm), rod diameter (from 16 to 24 mm), and rod-to-grain angle (parallel and perpendicular). Several different failure modes that are not commonly observed in the case of other applications of glued-in rods (e.g. failure between CLT layers) were obtained, especially in the case of greater glued-in lengths. It was found that these failure mechanisms can have a substantial effect on the ultimate load. A comparison of the experimental results with results obtained by using existing design equations showed that the latter tended to overestimate the ultimate loads in the case of specimens where the rod is placed parallel to the grain, and to underestimate them in the case of specimens where the rod is placed perpendicular to the grain. The existing design equations are therefore, in most cases, inappropriate for glued-in rods in CLT. However, the results of the study indicated that the equations could, potentially, be used as a basis for the definition of design expressions in the case of connections where there is no failure of the CLT cross sections (i.e. connections where the rod is placed parallel to the grain, and is in the middle of the CLT layer, where the rod diameter is small (≤12 mm) and the bonded-in length is short (≤120 mm)). The practical relevance of such small bonded-in rods is, however, in all probability, limited. It should be noted that, on the basis of the 60 tested specimens, it is still difficult to predict the general response of glued-in rods in CLT, since there are many possible influencing parameters which were either not investigated, or else investigated only to a limited extent (e.g. the rod-to-grain angle, the rod diameter, the glued-in length, the geometry of the connection, the CLT lay-up, and the position of the rod in the CLT cross-section).

The work presented in this paper is concerned with numerical simulations and parametric studies of glued-in rods in CLT. The numerical simulations are based on FE-analysis, and the input parameters were calibrated based on the above-described experimental study [23]. The FE-model consisted of linear elastic parts for the CLT laminations (i.e. structural timber boards, usually finger jointed, being part of timber layers in CLT) and for the steel rod, whereas the adhesive bond-line between the CLT laminations and the adhesive bond-line along the glued-in rod were modelled using a CZM approach. On the basis of the calibrated numerical model a parametric study was performed, where the glued-in length and the rod diameter were varied. In the last part of the study the behaviour of the connection in the case of different rod-to-grain angles was investigated. The research presented in this paper represents a first step towards the proposal of design equations which would take into account the unique response of glued-in rods in CLT.

2. Numerical modelling and description of the input parameters

2.1. 3D model description

The numerical model was defined so that it would be able to capture the different failure modes encountered during the experimental testing of glued-in rods in CLT [23]. The pull-pull test configuration shown in Fig. 1, with a threaded rod glued into the centre of the CLT cross section, was modelled using the FE software Abaqus VR2017 [24]. The loading was applied to the rod in a displacement controlled manner until complete failure occurred. In the case of the numerical models the same 5-layered CLT, without edge-bonding between the CLT laminations, was assumed, as in the experiments. The layer thicknesses were 33/20/34/20/33 mm and the lamination widths were 200 mm in the case of the thicker layers, and 120 mm in the case of the thinner layers. In the FE-model, symmetrical behaviour was assumed in all three directions. Altogether 10 different basic models for calibration with experiments were defined according to Table 1, with five different glued-in lengths and two different rod-to-grain angles for each glued-in length: parallel ($\alpha = 0°$) and perpendicular ($\alpha = 90°$) to the grain.

The differences between the parallel and perpendicular to the grain models were mainly in the basic geometry (Fig. 1). The axis of the glued-in rod is parallel to the wood fibre direction in the core (centric) layer of the 5-layered CLT for the parallel to grain model (Fig. 1a), and perpendicular to the wood fibre direction in the core layer for the perpendicular to grain model (Fig. 1b). In the case of

the perpendicular to grain models, a width of 50 mm was assumed for the edge laminations with grain orientation perpendicular to the rod axis. The total length of each model (L) was assumed to be the same as the length of the specimens in the experiments [23]. Each specimen length was defined according to the glued-in length of the rod (l_a).

The parts of the 3D model representing the C24 timber laminations were modelled as linear elastic and orthotropic with the stiffness properties presented in Table 2. The threaded rod was modelled as a linear elastic and isotropic steel part, with modulus of elasticity E = 210,000 MPa and Poisson's ratio v = 0.30. Similarly, the adhesive layer along the rod was modelled as a 2 mm thick linear elastic and isotropic part, with E = 2600 MPa and v = 0.25.

The face bonding of the timber laminations was modelled using a surface-to-surface interaction approach, including hard contact
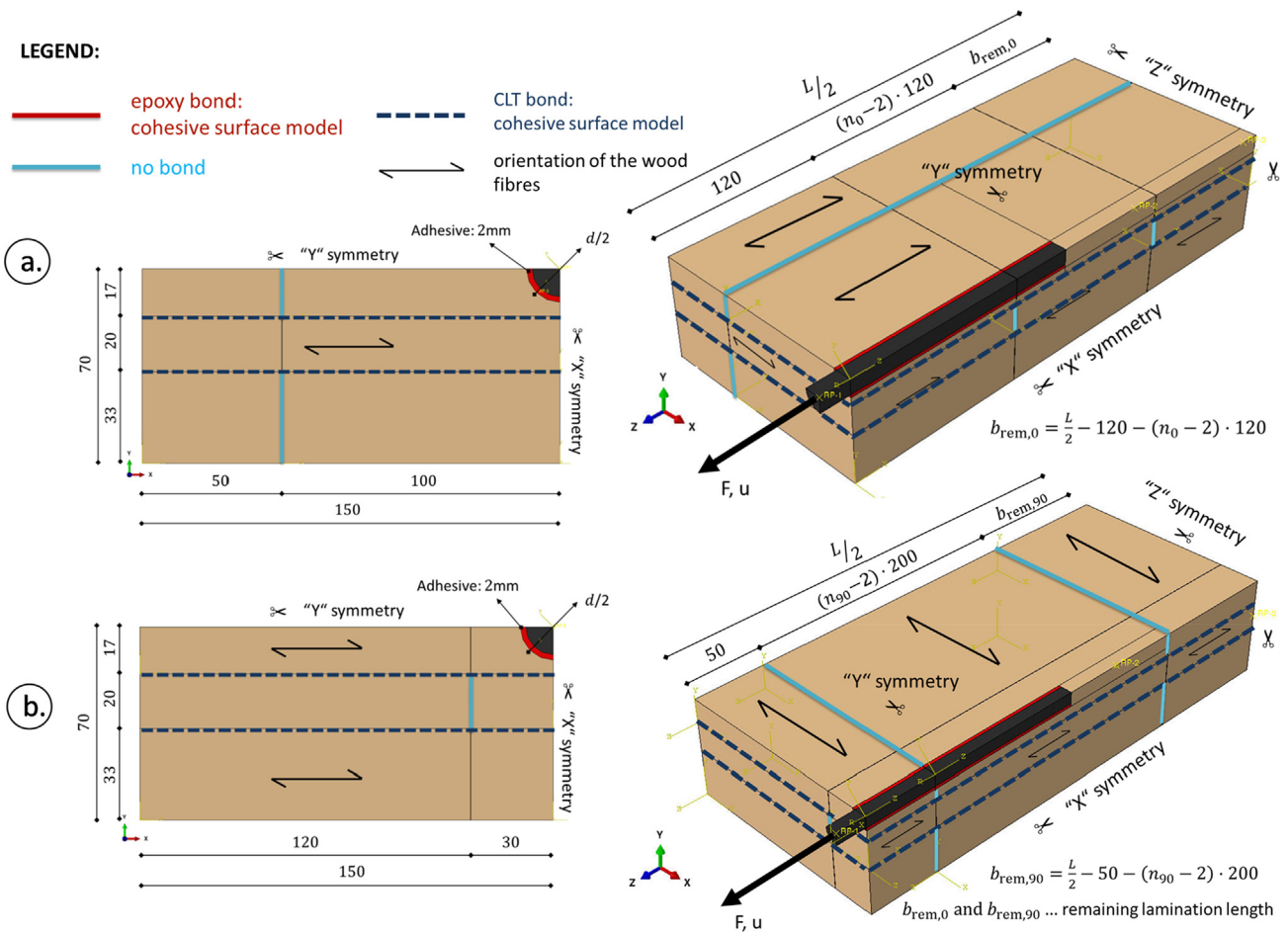
Table 1
Basic dimensions of the specimens which were used for calibration of the numerical models [23].

Specimen	L [mm]	n_0 [−]	n_{90} [−]	l_a [mm]	d_h [mm]	d [mm]
La80/	340	2	2	80	20	16
La160/	680	3	3	160	20	16
La240/	1020	5	4	240	20	16
La320/	1360	6	5	320	28	24
La400/	1700	8	6	400	28	24

Note: L = total specimen length (based on [23]), n_0 = number of transverse boards for the parallel to grain model, n_{90} = number of transverse boards for the perpendicular to grain model, l_a = glued-in length of the rod, d_h = hole diameter, d = rod diameter.

Fig. 1. Example of the basic model in Abaqus for calibration with the experiments: a. parallel and b. perpendicular to the grain model.

Table 2
Timber lamination stiffness properties.

	E_1 [MPa]	E_2 [MPa]	E_3 [MPa]	v_{12} [−]	v_{13} [−]	v_{23} [−]	G_{12} [MPa]	G_{13} [MPa]	G_{23} [MPa]
Spruce C24 (Picea abies)	11,000	370	370	0.40	0.40	0.45	690	690	50

Note: E_1, E_2, E_3... elastic moduli in the longitudinal, radial and tangential directions of the wood [25].
v_{12}, v_{13}, v_{23}...Poisson's ratios, where the first index refers to the direction of the applied stress and the second index to the direction of lateral deformation [26].
G_{12}, G_{13}, G_{23}... moduli of rigidity in the 12, 13 and 23 planes respectively [25].

in compression and nonlinear cohesive behaviour in tension perpendicular to the contact surfaces and in two shear directions parallel with the contact surfaces. A strain softening model with a damage initiation criterion based on the maximum nominal stress, and linear softening behaviour was assumed. The bond-line between the adhesive and the rod was modelled using a tie constraint, whereas the bond-line between the adhesive and the timber along the rod was modelled using the same type of surface-to-surface interaction approach as used for the flat-wise bonding between the timber laminations. The models were calibrated (see the next section) to the experimental test results by adjusting the value of the displacement at failure (δ_F) in order to achieve a good fit between experimental and numerical results in terms of global strength and stiffness. A viscosity coefficient $\eta = 0.005$ was applied for model stabilization. The calibrated model strength and stiffness parameters are presented in Table 3.

Since most of the experimentally observed failure modes directly involved the timber adhesive bond-line along the rod [23], a fine and regular mesh was used in these regions to model the rod and the epoxy adhesive. These elements exhibited aspect ratios close to 1:1:1 and the volumes of the elements ranged from 5 to 30 mm³, whereas the other elastic parts were modelled using a slightly coarser mesh (the volumes of these elements ranged from 50 to 200 mm³). A mesh sensitivity analysis was performed on one model with $l_a = 80$ mm and a rod parallel to the grain. The analysis showed that the difference in the global results was negligible (the difference in load capacity was less than 0.5%, and less than 5% for global stiffness) when the number of elements was doubled. The same linear 8-node elements with full integration (denoted C3D8 in Abaqus) were used for all parts of the models.

2.2. Description of the output variables

In order to compare and evaluate the results of the numerical parametric study and the results of the experimental tests, some specific output variables were defined as stated below.

(i) Ultimate tensile load [F_{ax}]: the maximum tensile force occurring during the loading.
(ii) The effective global stiffness [k_{eff}]: defined as the ratio $\frac{F_{40}-F_{10}}{u_{40}-u_{10}}$, where F_{40} and F_{10} are 40% and 10% of F_{ax}, respectively, and where u_{40} and u_{10} are the corresponding displacements at the loaded end of the rod. The global stiffness values determined for the numerical models ($k_{eff,0}$ and $k_{eff,90}$) were compared with the corresponding average stiffness values for each test series ($\bar{k}_{eff,0}$ and $\bar{k}_{eff,90}$).

(iii) Stiffness degradation (denoted as CSDMG in Abaqus) along the rod [T]: indicates the extension of damage in the adhesive bond-line between the rod and the CLT, at F_{ax}. T [−] is defined as the proportion of the timber-adhesive bond-line along the rod that has experienced damage initiation and stiffness degradation, where $T = 0$ corresponds to a state of no damage and pure linear elastic behaviour of the complete bond-line area, and $T = 1.0$ corresponds to a state where damage initiation has occurred over the complete bond-line area.

(iv) Stiffness degradation (CSDMG) between CLT layers [Γ]: indicates the extension of damage in the flat-wise bonding between the timber laminations, at F_{ax}. Γ [−] is defined as the proportion of the bonded area that has experienced damage initiation and stiffness degradation, where $\Gamma = 0$ corresponds to a state of no damage and pure linear elastic behaviour of the complete bonded area, and $\Gamma = 1.0$ corresponds to a state where damage initiation has occurred over the complete bonded area. Different reference areas are considered for the parallel and perpendicular to grain models (Fig. 1): Γ_0 relates to the parallel to grain models and a reference area of 120×150 mm² while Γ_{90} relates to the perpendicular to grain models and a reference area of 250×150 mm².

Variables (i) and (ii) are available from the numerical results as well as from the experimental tests, whereas variables (iii) and (iv) are defined in order to enable comparisons between the numerical analyses only.

3. Calibration of the 3D model with experimental data

Some of the input parameters for the FE-model were calibrated to the results of the experimental study [23], whereas the other input parameters were set according to values found in the literature. The timber lamination stiffness parameters according to Table 2 were used for all the analyses, without any calibration to

Table 3
Properties for the cohesive surfaces: timber-adhesive bond-line along the rod and flat-wise bonding of the timber laminations.

	σ [MPa]	τ_1 [MPa]	τ_2 [MPa]	K_{nn} [N/mm³]	$K_{tt,1}$ [N/mm³]	$K_{tt,2}$ [N/mm³]	δ_f [mm]	η [−]
Timber adhesive bond-line along rod (0° model)	5	10.9	10.9	1300	500	500	0.1	0.005
Timber adhesive bond-line along rod (90° model)	5	10.9	10.9	1300	500	500	5.5	0.005
Flat-wise bonding between timber laminations	5	1.5	1.5	500	500	500	1.5	0.005

Note: σ ... strength in the normal direction, limited by the perpendicular to the grain tensile strength of spruce [27,28].
τ_1, τ_2 ... shear strengths; based on [23,29] for the surface along the rod and limited to the rolling shear properties of CLT [30,31].
K_{nn} ... stiffness in the normal direction [32].
$K_{tt,1}$, $K_{tt,2}$ ... stiffness in the shear directions [32].
δ_f ... displacement at failure (calibrated value).
η ... viscosity coefficient (a sufficiently small value to have a negligible effect on the final result).

the experimental results. The tensile strength σ (stress perpendicular to the bond-line) was assumed to be equal for all the adhesive bond-lines (Table 3), corresponding to an assumed timber strength in tension perpendicular to the grain [27,28]. The in-plane shear strengths τ_1 and τ_2 of the timber-to-timber bond-line were assigned fixed values according to Table 3, corresponding to assumed rolling shear strength of the timber laminations [30,31]. The stiffness parameters of the flat-wise bonding between the laminations were further assigned the values given in Table 3, which are similar to the values used for the FE-analyses of CLT beams presented in [32].

The shear strengths τ_1 and τ_2 of the timber-adhesive bond-line along the rod were determined based on the experimentally found strengths with specimens with the rod placed parallel to the grain and having a bonded-in length of l_a = 80 mm [23]. The value found (10.9 MPa), was higher than the expected timber strength. Such high values have, however, also been confirmed in other studies [29], and can be explained by the fact that the strength represents the local strength (at a material point), and possibly to some extent also by the state of stress at failure, in which frictional forces also play a role at pull-out.

In order to capture the difference in the response observed in the experiments for the two specimen types, different values of the displacement at failure δ_f were assumed for the timber adhesive bond-line along the rod for the parallel to grain models and for the perpendicular to grain models, respectively (Table 3). These values were determined based on a calibration to the experimentally found responses of the specimens with different bonded-in lengths, considering rod placements parallel and perpendicular to the grain, respectively. The displacement at failure is a mechanical model characteristic, which is difficult to obtain experimentally, and information in the scientific literature on the specific epoxy adhesive and the bond-lines oriented according to different wood-to-grain angles could not be obtained. During calibration of the parallel and perpendicular to the grain models, the sensitivity of their prediction to changes of the value δ_f was investigated. The investigation involved different values of δ_f, ranging from 0.05 to 11. In the experiments, the parallel to the grain specimen failed in a brittle manner. When calibrating the parallel to the grain models, δ_f = 0.1 yielded brittle failure and also the smallest difference between the predicted and experimentally determined average capacity of each test series. For the perpendicular to the grain models, values of δ_f between 1.5 and 11 influenced the bearing capacity only by approximately 10%, so that an intermediate value of 5.5 mm was chosen (Table 3). This value was also found to provide good agreement regarding the shape of the force-displacement curves after reaching maximum load (in the post-failure part of the curve). Using the above-described approach during calibration it is thus clear that it was assumed that the bond-line between the rod and the CLT had the same strength irrespective of the rod-to-grain angle. This is obviously a simplification. Furthermore, for the case of a perpendicular rod, shear along the rod is transferred partly as longitudinal/transverse shear and partly as rolling shear, depending on the position in the circumferential direction, and thus a varying strength could be expected in that circumferential direction. In order to keep the model simplified, these characteristics were not modelled.

The results in terms of the load vs. rod displacement relationship of the experimental tests and the corresponding FE-analysis are shown in Fig. 2. In general, the experimental and numerical results agree well, although some deviations can be observed:

– For the parallel to grain models, the ultimate tensile load $F_{ax,0}$ and the effective global stiffness $k_{eff,0}$ are in general overestimated compared to the mean experimental results.

– For the perpendicular to grain models, the ultimate tensile load $F_{ax,90}$ is slightly overestimated, whereas the effective global stiffness $k_{eff,90}$ is in most cases slightly underestimated compared to the mean experimental results.

A possible error source in the calibration process is the simplified approach as regards the bond-line properties in the circumferential direction mentioned above. However, it was not deemed meaningful to introduce additional parameters into the model since these would be very difficult to verify. Another error source could be the assumption of linear elastic behaviour of the timber laminations in the numerical analyses. The results of the experiments presented in [23] showed that some failure modes included a fracture within the timber laminations. Although different failure modes occurred within each test series, this proved to have negligible effect on the average capacity values [23]. Nevertheless, the numerical modelling could be further improved by introducing nonlinear behaviour of the timber laminations and taking into account a broader variety of glued-in rod connections in the CLT, which were not considered in this paper (e.g. connections with the rod placed between the two CLT layers, the use of CLT with bonded lamination edges etc.).

4. Parametric studies

4.1. Rod diameter and glued-in length

The calibrated numerical models were further used for parametric studies, whose main objective was to investigate the response of the glued-in rod connections for different rod diameters and different glued-in lengths. The rod diameter d was varied between 4 and 28 mm, in steps of 2 mm. The thickness of the adhesive layer was set to 2 mm for all models, the same value as used in the experiments [23]. The same glued-in lengths as used in the experiments (l_a = 80, 160, 240, 320 and 400 mm) were also taken into account for the parametric studies. The results for the parallel to grain models and the perpendicular to grain models, in terms of the influence of the glued-in length l_a and the rod diameter d on the output variables $F_{ax,0}$, Γ_0, and T_0, are shown in Figs. 3 and 4, respectively. It should be noted that the glued-in rods were modelled as linear elastic in the numerical analyses, so that the results do not include any rod yielding or failure. The load-carrying capacity of the steel rod, assuming steel of grade 10.9, is indicated by the dotted lines in Figs. 3 and 4. As can be seen in Fig. 4, the capacity of such a rod was in some cases smaller than that of the adhesive bond-lines.

The results of the numerical analyses show a comparatively low degree of damage between the CLT laminations for the parallel to grain models, with $\Gamma_0 \leq 0.20$ for all analyses, meaning that 20% or less of the observed surface between the CLT laminations has experienced damage initiation and stiffness degradation when reaching the respective maximum loads. In the analyses, no shear failure between the CLT laminations was observed for rod diameters $d \leq 14$ mm. The analyses furthermore predict the extension of damage in the flat-wise bonding between the CLT laminations to increase for larger rod diameters and greater bonded-in lengths. These findings agree well with the experimental results presented in [23].

As expected, the maximum tensile load $F_{ax,0}$ increased with the rod diameter and the glued-in length. However, after a certain size of rod diameter has been reached, $F_{ax,0}$ does not increase substantially with further increase in the rod diameter. For example, the difference in $F_{ax,0}$ between the glued-in rod diameters 20 mm and 26 mm is only 5% for the parallel to grain models with l_a = 240 mm (Fig. 3). This relationship is connected to the output
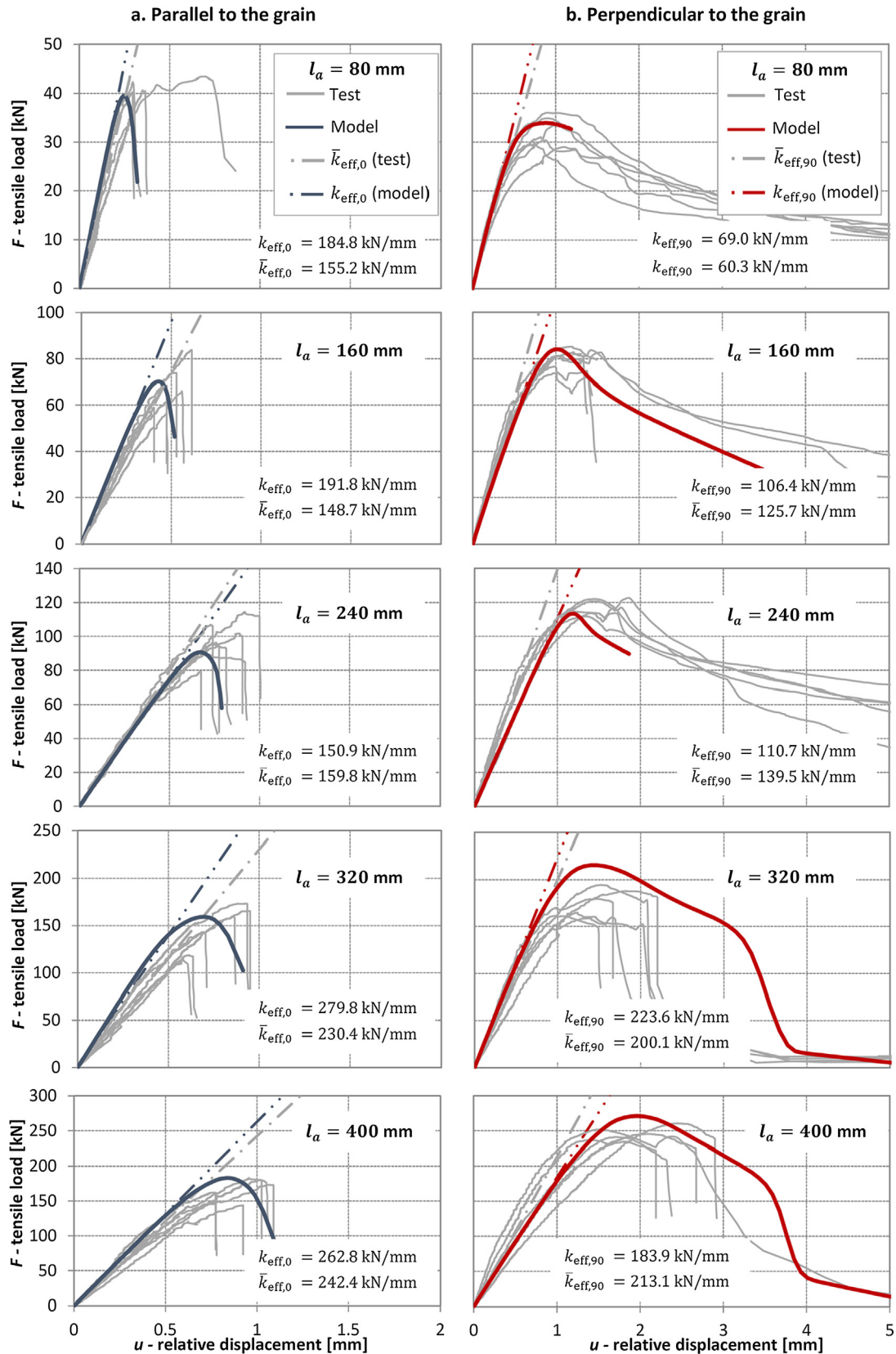
a. Parallel to the grain

b. Perpendicular to the grain

Fig. 2. Load vs. rod displacement response of the calibrated numerical models (coloured curves) and the experimental tests (grayscale curves). (For interpretation of the references to color in this figure legend, the reader is referred to the web version of this article.)
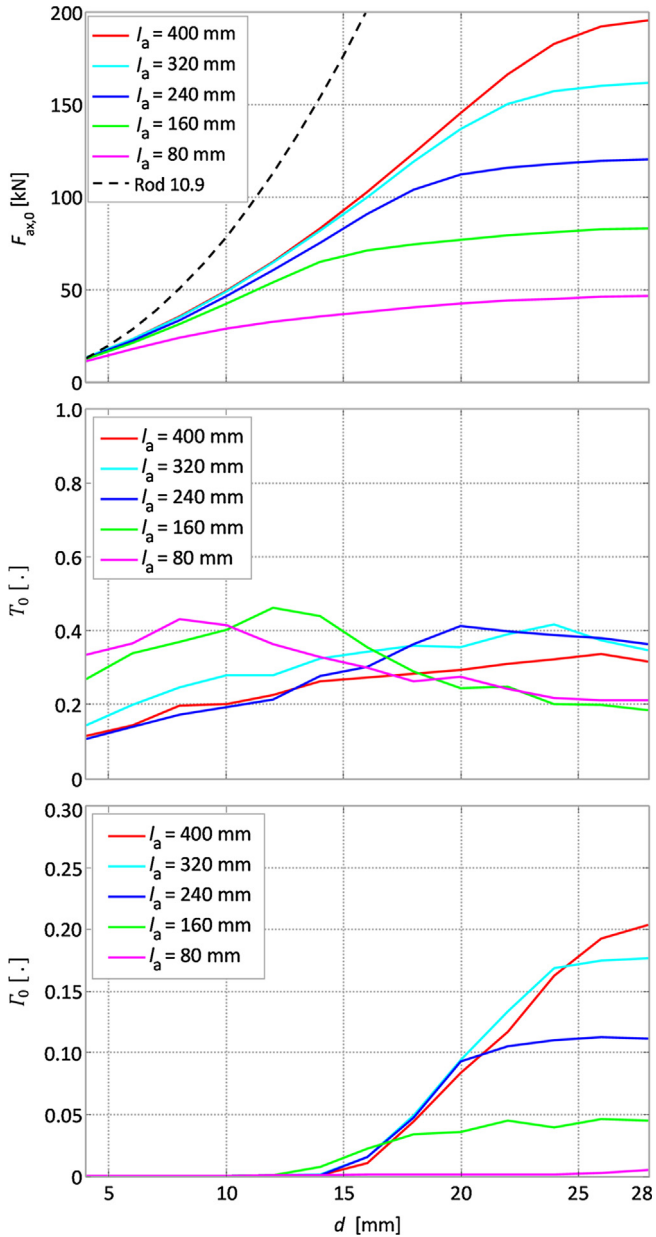
Fig. 3. The maximum tensile load ($F_{ax,0}$) and damage parameters for the timber-adhesive contact surface along the rod (T_0) and the contact surface between the timber laminations (Γ_0), depending on the glued-in rod diameter (d) and the glued-in length (l_a) for the parallel to grain models.

Fig. 4. The maximum tensile load ($F_{ax,90}$) and damage parameters for the timber-adhesive contact surface along the rod (T_{90}) and the contact surface between the timber laminations (Γ_{90}), depending on the glued-in rod diameter (d) and the glued-in length (l_a) for the perpendicular to grain models.

parameter Γ_0 which indicates the extension of damage between the CLT laminations. As can be seen in Fig. 3, the shape of the curves representing $F_{ax,0}$ and Γ_0 are similar, and the maximum tensile load $F_{ax,0}$ is reached at approximately the maximum value of Γ_0.

The parameter T_0, indicating the extension of damage in the adhesive bond-line along the rod, varied between 0.20 and 0.40 for the analyses of the parallel to grain models presented in Fig. 3. For small rod diameters T_0 was much higher than Γ_0. However, the parameter Γ_0 clearly increases with increasing rod diameter whereas the parameter T_0 is fairly constant or decreases slightly. An interpretation of this is that, for increasing rod diameters, the failure mode is more dominated by failure between the CLT laminations, and less by pull-out of the glued-in rod.

The results obtained for the perpendicular to grain models (Fig. 4) are, in general, similar to those obtained for the parallel
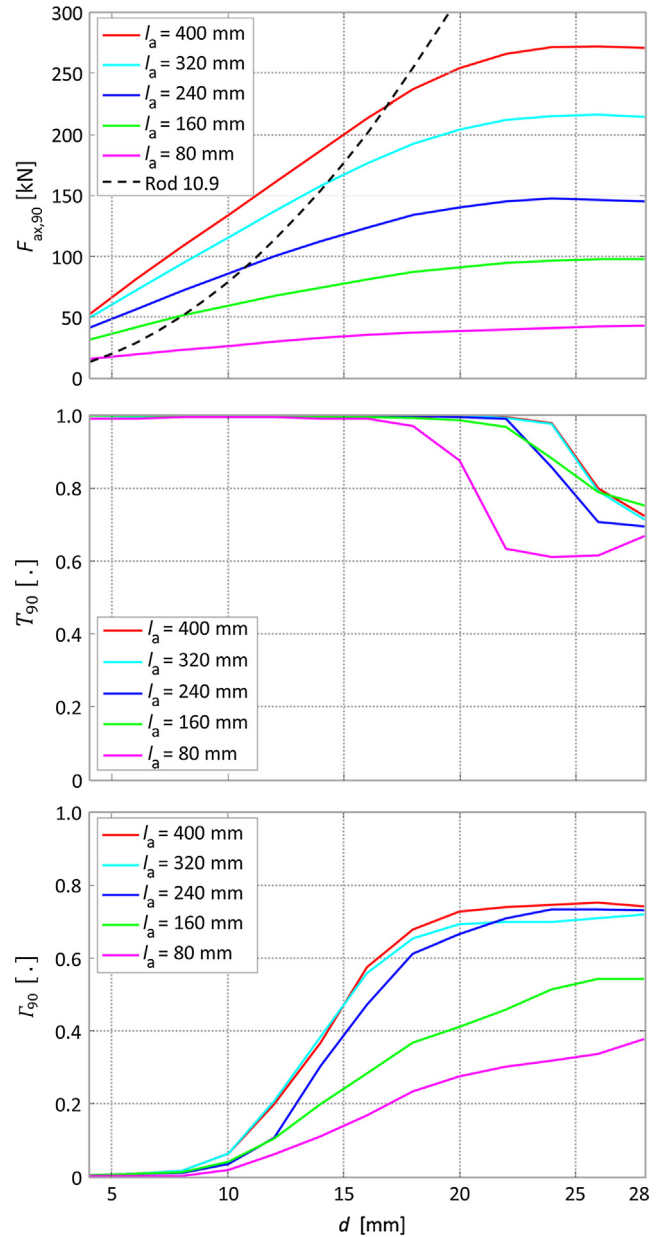
to grain models (Fig. 3): larger rod diameters and larger bonded-in lengths yield higher ultimate tensile loads $F_{ax,90}$. Similarly, $F_{ax,90}$ is related to the output parameter Γ_{90} and there is an optimal rod diameter for each glued-in length beyond which there is no significant increase in the load-bearing capacity. However, there is a significant difference between the parallel and perpendicular to grain models, which relates to the extent of damage in the bond-line along the rod (T_{90}) and the bond-line between the CLT laminations (Γ_{90}). The parameter Γ_{90} is, in general, larger for the perpendicular to grain models compared to the parallel to grain models. For rod diameters d = 20–28 mm and glued-in lengths l_a = 240–400 mm the values of Γ_{90} are within the range of 0.65–0.75. For the parallel to grain models, the values of Γ_0 range from 0 to about 0.20 for all the rod diameters and glued-in lengths. It should be noted that the absolute values of Γ_0 and Γ_{90} are not directly comparable, since different definitions of the considered

reference areas are used for the two different types of models (Section 2.2).

Damage in the surface between the CLT laminations (Γ_{90}) appears in the case of rod diameters larger than about 10 mm. The extent of damage in the bond-line along the rod (T_{90}) is almost 100% for rod diameters $d \leq 16$ mm, but reduces to 60–80% for larger diameters. This can be explained as follows: when larger diameters are used, a larger load is applied to the adhesive surfaces between the CLT laminations. Additionally, the distance between the rod's circumferential surface and the adhesive layer between two CLT laminations decreases, which means that, at a given load level, the shear stress is greater at the location of the adhesive layer between the CLT laminations and also more concentrated to the area closer to the rod, thus inducing damage over a larger part of the reference area considered.

The results of the parametric study indicate a higher load-bearing capacity for the perpendicular to grain models compared to the parallel to grain models. This result applies to all rod lengths, and was also confirmed by the experiments [23]. Large differences between the rod orientations were also found for the output parameters Γ and T, which describe the extension of damage in the bond-lines between the CLT laminations and the bond-line along the rod. In general, the extension of damage at the ultimate tensile loads of the perpendicular to grain models was higher compared to the corresponding parallel to grain model. This result is in line with the observations during the experiments where a difference in failure mechanisms [23] was seen. The experiments showed that the perpendicular to grain specimens failed mainly at the bond-lines between the CLT laminations (adhesive failure or rolling shear failure), whereas the parallel to grain specimens failed mainly at the timber-adhesive bond-line along the glued-in rod. In general, this experimental finding fits well with the numerically determined values of the damage parameters Γ and T.

4.2. Rod-to-grain angle

The main aim of the second parametric study was to investigate the axial response for the case when the rod is glued at different angles to the grain direction of the core layer of the CLT element. There are several applications in which such a rod orientation could be useful, e.g. at connections between a steel frame and a CLT infill [5]. The results of the experiments presented in [23], as well as those obtained from the numerical analyses presented in Section 4.1, showed a significant difference between the parallel to grain models and the perpendicular to grain models, possibly also indicating a major influence on the connection's load-carrying capacity for intermediate rod-to-grain angles.

In order to capture the connection response at any rod-to-grain angle in a reasonably convenient manner, the 3D model described in Section 2 was simplified. The simplified numerical model was assembled with individual parts representing each CLT layer, as illustrated in Fig. 5. It was assumed that the individual laminations within the respective layers were perfectly bonded along their narrow faces. With this approach, the ultimate tensile load is probably overestimated since the failure mode associated with complete lamination tear-out is restricted. The cohesive surfaces modelling the flat-wise adhesive bond-line between the CLT layers and timber-adhesive bond-line along the rod were defined using the same input parameters as described in Section 4.1, and are given in Table 3. Different values of the displacement at failure δ_f were used for the analyses of the parallel and perpendicular to grain models, as presented in Section 4.1. For the here considered numerical analyses of intermediate rod-to-grain angles, the displacement at failure for the timber-adhesive bond-line along the rod was linearly interpolated from $\delta_f = 0.1$ for the 0° model to $\delta_f = 5.5$ mm for the 90° model. The same type of analysis as
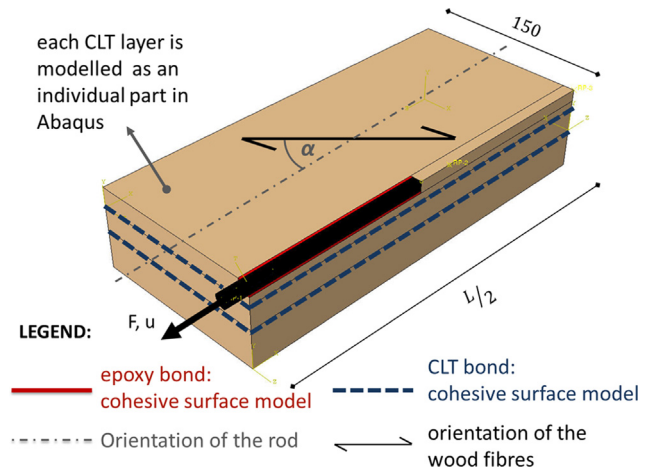

Fig. 5. Geometry and description of the simplified 3D FE model for the parametrization of the rod-to-grain angle (α).

described in Section 2, with monotonic static loading, was performed also for the here considered simplified models.

The load vs. displacement responses for each of the considered rod-to-grain angles are shown in Fig. 6 for the models with a glued-in length of $l_a = 160$ mm and a rod diameter of $d = 16$ mm. The results indicate that the behaviour for larger rod-to-grain angles α is more ductile compared to the 0° model. This is partly a consequence of the different assumed values for the displacement at failure δ_f for the different models, and also a consequence of the lower effective global stiffness k_{eff} of the models with a larger rod-to-grain angle α.

The results of the simplified model (Fig. 6) and the more complex model (Fig. 2 and Fig. 3) agree, as expected, rather well for rod orientations parallel to the grain ($\alpha = 0°$). The predicted ultimate loads for the two respective models are 85 kN and 70 kN, corresponding to a 21% increase for the simplified model compared to the more complex model. For rod orientations perpendicular to the grain ($\alpha = 90°$), the corresponding ultimate loads for the two respective models are 110 kN and 85 kN, giving a relative difference of 29%. The difference in the predicted ultimate tensile loads between the simplified and more complex models is expected to decrease for shorter glued-in lengths and to increase for longer glued-in lengths.

The maximum obtained tensile load F_{ax} as influenced by the rod-to-grain angle α is shown in Fig. 7, for glued-in lengths $l_a = 80$ and 160 mm. It can be seen that minimum values of F_{ax} are obtained for a rod orientation parallel to grain ($\alpha = 0°$) for both the glued-in lengths considered. The load F_{ax} then increases with the angle α until a maximum value is reached at $\alpha \approx 20–30°$. As the angle α is further increased, there is a drop in the ultimate load, which reaches a local minimum at $\alpha \approx 60°$ before increasing again with a further increase in the rod-to-grain angle. Similar results were obtained also in the case of the experimental tests of glued-in rods in CLT reported in [5].

Fig. 8 shows the effective global stiffness k_{eff} as influenced by the rod-to-grain angle α for the glued-in lengths $l_a = 80$ and 160 mm. It should be noted that the parameter k_{eff} is the global effective stiffness of the complete connection (including the steel rod, the adhesive layers, and the CLT, explained in Section 2.2), and should therefore not be confused with the CLT stiffness. The results show that k_{eff} increases slightly with increasing α between 0° and 15°, the maximum stiffness occurring at $\alpha = 15°$. With a further increase in the rod-to-grain angle α, a gradual drop in stiffness occurs, and the minimum stiffness is obtained for $\alpha = 90°$. This decrease in stiffness with the angle α is mainly related to the
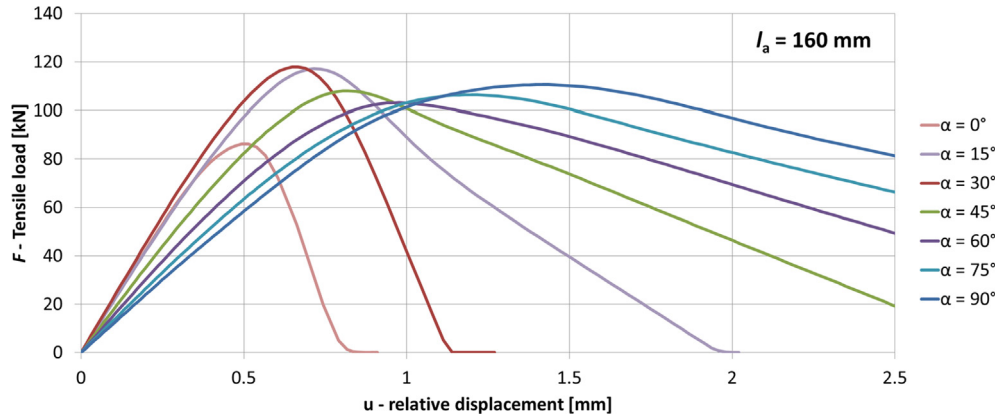
Fig. 6. Load vs. rod displacement response for different rod-to-grain angles, for a bonded-in length l_a = 160 mm and a rod diameter d = 16 mm.
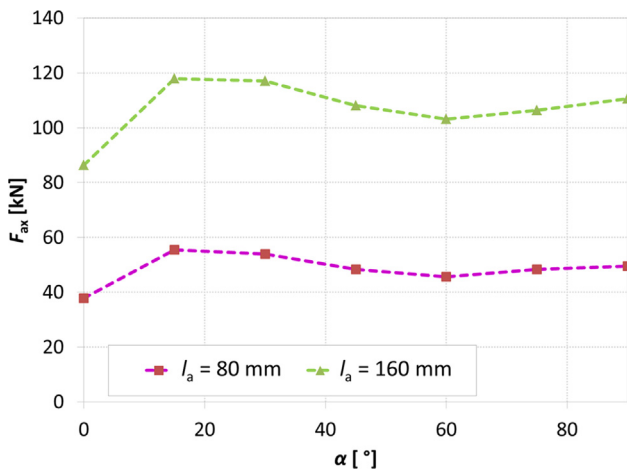

Fig. 7. Ultimate axial load F_{ax} for glued-in rod lengths of l_a = 80 and 160 mm plotted against the rod-to-grain angle α.
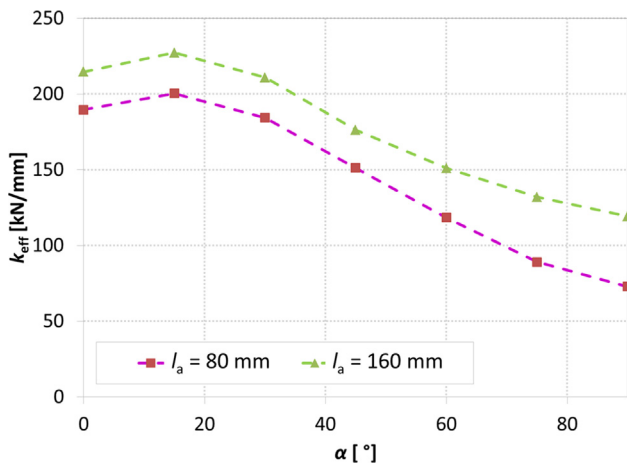

Fig. 8. Effective global stiffness k_{eff} for glued-in rod lengths of l_a = 80 and 160 mm plotted against the rod-to-grain angle α.

stiffness of the CLT element itself, and hence related not only to the angle α but also to the number of CLT layers and the individual lamination thicknesses. In general, a similar relationship between the global effective stiffness and the angle α can be expected (i.e. a decrease in stiffness with α) for all CLT panels, although the absolute values will vary depending on the analysed CLT lay-up.

4.3. Commentary on the design equations

Over the years, starting as long ago as in the 1980's, a lot of research has been done on glued-in rods. Often the aim has been to provide the information required to prepare standards (design approaches, code models) that would allow an increased, more advanced and more reliable use of glued-in rods in timber structures [33]. A comparison of design equations derived for other glued-in rod applications (e.g. structural timber and glulam) with the experimental results of glued-in rods in CLT was performed in [23]. The so far derived design equations for the prediction of the pull-out capacity of single glued-in rods are in general similar, where the basic influencing parameters concern the geometry of the connection including typically the anchorage length and rod diameter, sometimes also in combination with the slenderness ratio (the ratio of the anchorage length to the drill-hole diameter). Additionally, some equations include the volume of the adhesive, which depends on the anchorage length and the glue line thickness; the type of adhesive used (brittle or ductile); the density and modulus of elasticity of the wood; the rod-to-grain orientation (only parallel and perpendicular variants are considered); the bar type (threaded rod, steel reinforcement bar, other materials, etc.), and other factors.

The results of the parametric analyses presented here showed that a design equation for glued-in rod connections in CLT must include also other parameters, such as: the orientation of the rod (Figs. 6–8) and the rod diameter size in relation to the size of the CLT layer within which the rod is glued (Figs. 3 and 4). The influence of these parameters could be added to existing equations by introducing additional coefficients. For example, it can be seen from Figs. 6 and 7 that the capacity of the connection increases/ decreases by changing α from 0° to 90°. The same trend of results could be included as a coefficient to differently weight the design capacity calculated by means of the already established design equations. Similarly, the influence of the size of the rod in relation to the CLT layer thickness could be taken into account quantitatively by comparing the parameters Γ and T.

On the basis of the performed analyses it can be assumed that the other parameters, which were not included in the study, could have a strong effect on the pull-out capacity of a single rod: (i) position of the rod in relation to the CLT layers, (ii) the CLT geometry and its material characteristics, (iii) the edge gluing of the CLT laminations, (iv) the edge distance of the rod and the outer CLT layer etc. For example, the rod can be glued in the middle of a single layer (as was assumed in this study), in between two neighbouring layers, next to the border of the CLT layer or even close to the CLT edge. Consequently, the rod can be glued into the CLT at a position where it will interact with two layers with different

grain orientations and, consequently, the pull-out response will be influenced, as has been shown in this study (Figs. 6 and 7). The influence of these effects needs to be further explored in order to revise the design equations or propose new ones.

5. Summary and conclusions

The paper deals with numerical simulations and parametric studies of glued-in rods in cross laminated timber (CLT). The considered FE-model was based on the assumption of linear elastic behaviour of the timber laminations, the steel rod, and the adhesive, whereas a strain softening cohesive surface approach was used for the bond-lines between the timber laminations and for the interface between the adhesive and the wood along the rod. This modelling approach offers the possibility of studying different failure modes for glued-in rods in CLT, as encountered in previous tests [23]. The model input parameters were calibrated to experimental results of specimens with rod orientations parallel and perpendicular to the grain and having different glued-in lengths. In general, good agreement was obtained between the results for the FE-analyses and the experimental tests presented in [23], both with regard to load-bearing capacity and connection stiffness, for all the considered geometries, as is presented in Fig. 2.

The numerical parametric studies concerning the influence of the glued-in length and the rod diameter are presented in Section 4.1 for rod orientations parallel or perpendicular to the grain, using the calibrated model input parameters. Larger load-bearing capacities were, in general, found for rod orientation perpendicular to the grain, a finding which agrees well with the experimental results [23]. The numerical results further show, as expected, that the connection's load-bearing capacity generally increases with the glued-in length and the rod diameter. However, the increase in global axial load-bearing capacity for each rod orientation and each glued-in length occurs only up to a certain rod diameter, as can be seen in Figs. 3 and 4. A further increase in the rod diameter, above this value, has only a very small influence on the global axial load-bearing capacity. This behaviour is also related to a shift in failure modes, with the bond-lines between the timber laminations being comparatively more stressed and the bond-line along the rod being comparatively less stressed, at the increased rod dimension. In the numerical simulations this is reflected by a larger degree of damage within the bond-lines between the timber laminations for larger rod diameters, at the moment of maximum load. A general difference in failure modes was also found between the perpendicular and parallel to grain models, where the perpendicular to grain models fail to a significantly larger degree due to the highly stressed bond-lines between the timber laminations. This result, too, is in-line with the experimental observations reported in [23]. It should however be noted that this result is valid for the analysed examples with the rod in the central position of the CLT cross-section and with a diameter smaller than the lamination thickness. In cases when the rod would cross two or even more layers this trend of results could change significantly.

Numerical parametric studies concerning the influence of the rod-to-grain angle α are presented in Section 4.2, considering angles $\alpha = 0°$, 15°, 30°, 45°, 60°, 75° and 90° and a geometrically simplified FE-model. The numerical simulations indicate that the maximum global axial load-bearing capacity and stiffness cannot be expected either for a rod orientation parallel to the grain ($\alpha = 0°$) or perpendicular to the grain ($\alpha = 90°$), but for an intermediate rod-to-grain angle of approximately $\alpha = 20°$.

The mechanical behaviour of glued-in rod connections in CLT is very complex, as is reflected by the many different failure modes obtained in experimental tests [23] and further emphasized when moving into advanced 3D numerical modelling. The mechanical

behaviour is influenced by numerous geometrical and material property parameters and by several potential failure zones, which makes numerical modelling a challenging task. The high potential of using glued-in rod connections for CLT structures in terms of, for example, mechanical properties, costs, and aesthetics is however believed to be significant. This motivates further research efforts in this field. As regards the numerical models used within the work presented here, possible improvements include consideration of nonlinear material behaviour also for the timber laminations and the steel rods, as well as further development of the cohesive surface approach used to describe the bond-lines between the CLT laminations and the interface between the adhesive and the laminations along the rod.

Conflict of interest

The authors declare that they have no conflict of interest.

Ethical approval

The authors declare that there is no issue concerning ethical standards.

Informed consent

Informed consent was obtained from all individual participants included in the study.

Acknowledgements

References

[1] H. Riberholt, Glued bolts in Glulam. Report R210, Department of Structural Engineering, Technical University of Denmark, Lyngby, Denmark, 1986.

[2] J. Kangas, Joints of glulam structures based on glued-in ribbed steel rods, Technical Res. Centre Finland (1994).

[3] J. Ehlbeck, W. Siebert, Praktikable Einleimmethoden und Wirkungsweise von eingeleimten Gewindestangen unter Axialbelastung bei Übertragung von großen Kräften und bei Aufnahme von Querzugkräften in Biegeträgern: Einleimmethoden, Haftspannungsverlauf, Meßverfahren, IRB-Verlag, 1987.

[4] M. Andersen, M. Høier, Glued-in Rods in Cross Laminated Timber, Master's Thesis, Aarhus University, 2016.

[5] R.J. Koets, Hoogbouw met cross laminated timber literatuur-, numeriek- en experimenteel (vervolg-) onderzoek naar CLT infilled frames, Master Thesis, Eindhoven University of Technology, 2012.

[6] J. Müller, W. von Roth, Untersuchungen zum Tragverhalten zur Faser in Nadelholz eingeleimte Stäben aus unterschiedlichen Materialen, Holz Als Roh Werkst. 49 (1991) 85–90.

[7] S. Aicher, L. Höfflin, M. Wolf, Influence of specimen geometry on stress distributions in pull-out tests of glued-in steel rods in wood, Otto-Graf-J. 9 (1998) 205.

[8] S. Aicher, M. Wolf, G. Dill-Langer, Heat flow in a glulam joist with a glued-in steel rod subjected to variable ambient temperature, Otto-Graf-J. 9 (1998) 185.

[9] J. Broughton, A. Hutchinson, Pull-out behaviour of steel rods bonded into timber, Mater. Struct. 34 (2001) 100–109, https://doi.org/10.1007/BF02481558.

[10] C.J. Johansson, E. Serrano, P.J. Gustafsson, B. Enquist, Axial strength of glued in bolts – calculation model based on non linear fracture mechanics – a preliminary study, Int. Counc. Build. Res. Stud. Doc. Work. Comm. W18—Timber Struct. Meet. (1995).

[11] E. Serrano, Glued-in rods for timber structures – a 3D model and finite element parameter studies, Int. J. Adhes. Adhes. 21 (2001) 115–127, https://doi.org/10.1016/S0143-7496(00)00043-9.

[12] E. Serrano, P.J. Gustafsson, Fracture mechanics in timber engineering – strength analyses of components and joints, Mater. Struct. 40 (2007) 87–96, https://doi.org/10.1617/s11527-006-9121-0.

[13] M. del Senno, M. Piazza, R. Tomasi, Axial glued-in steel timber joints – experimental and numerical analysis, Holz Als Roh Werkst. 62 (2004) 137–146, https://doi.org/10.1007/s00107-003-0450-1.

[14] V. Gardelle, P. Morlier, Geometric parameters which affect the short term resistance of an axially loaded glued-in rod, Mater. Struct. 40 (2007) 127–138, https://doi.org/10.1617/s11527-006-9155-3.

[15] E. Martín, J. Estévez, D. Otero, Influence of geometric and mechanical parameters on stress states caused by threaded rods glued in wood, Eur. J. Wood Wood Prod. 71 (2013) 259–266, https://doi.org/10.1007/s00107-013-0678-3.

[16] J. Lartigau, J.-L. Coureau, S. Morel, P. Galimard, E. Maurin, Mixed mode fracture of glued-in rods in timber structures, Int. J. Fract. 192 (2015) 71–86, https://doi.org/10.1007/s10704-014-9986-9.

[17] K.-U. Schober, T. Tannert, Hybrid connections for timber structures, Eur. J. Wood Wood Prod. 74 (2016) 369–377, https://doi.org/10.1007/s00107-016-1024-3.

[18] M. Madhoushi, M.P. Ansell, Effect of glue-line thickness on pull-out behavior of glued-in GFRP rods in LVL: finite element analysis, Polym. Test. 62 (2017) 196–202, https://doi.org/10.1016/j.polymertesting.2017.06.029.

[19] C. Grunwald, T. Vallée, S. Fecht, O. Bletz-Mühldorfer, F. Diehl, L. Bathon, F. Walther, R. Scholz, S. Myslicki, Rods glued in engineered hardwood products Part II: numerical modelling and capacity prediction, Int. J. Adhes. Adhes. (2018), https://doi.org/10.1016/j.ijadhadh.2018.05.004.

[20] M. Cepelka, K.A. Malo, H. Stamatopoulos, Effect of rod-to-grain angle on capacity and stiffness of axially and laterally loaded long threaded rods in timber joints, Eur. J. Wood Wood Prod. 76 (2018) 1311–1322, https://doi.org/10.1007/s00107-018-1314-z.

[21] H. Stamatopoulos, K.A. Malo, Withdrawal of pairs of threaded rods with small edge distances and spacings, Eur. J. Wood Wood Prod. 76 (2018) 31–42, https://doi.org/10.1007/s00107-016-1146-7.

[22] H. Mpidi Bita, T. Tannert, Numerical optimisation of novel connection for cross-laminated timber buildings, Eng. Struct. 175 (2018) 273–283, https://doi.org/10.1016/j.engstruct.2018.08.020.

[23] B. Azinović, E. Serrano, M. Kramar, T. Pazlar, Experimental investigation of the axial strength of glued-in rods in cross laminated timber, Mater. Struct. 51 (2018), https://doi.org/10.1617/s11527-018-1268-y.

[24] Hibbitt, ABAQUS/standard: User's Manual, Karlsson & Sorensen Inc, 2017.

[25] C. Sandhaas, Mechanical behaviour of timber joints with slotted-in steel plates, (2012).

[26] CEN, EN 338:2016 Structural timber - strength classes, 2016.

[27] P. Niemz, W. Sonderegger, Holzphysik: Physik des Holzes und der Holzwerkstoffe, Carl Hanser Verlag GmbH Co KG, 2017.

[28] K.B. Dahl, Mechanical properties of clear wood from Norway spruce Doctoral thesis, Department of Structural Engineering, Norwegian University, 2009.

[29] E. Serrano, Glued-in rods for timber structures – an experimental study of softening behaviour, Mater. Struct. 34 (2001) 228–234.

[30] K.B. Dahl, K.A. Malo, Nonlinear shear properties of spruce softwood: numerical analyses of experimental results, Compos. Sci. Technol. 69 (2009) 2144–2151.

[31] T. Ehrhart, R. Brandner, G. Schickhofer, A. Frangi, Rolling shear properties of some european timber species with focus on cross laminated timber (CLT): Test configuration and parameter study, in: Int. Netw. Timber Eng. Res. Proc. Meet., Timber Scientific Publishing, KIT Holzbau und Baukonstruktionen, 2015, pp. 61–76.

[32] H. Danielsson, M. Jeleč, E. Serrano, V. Rajčić, Cross laminated timber at in-plane beam loading – comparison of model predictions and FE-analyses, Eng. Struct. 179 (2019) 246–254, https://doi.org/10.1016/j.engstruct.2018.10.068.

[33] M. Stepinac, F. Hunger, R. Tomasi, E. Serrano, V. Rajcic, J.-W. van de Kuilen, Comparison of design rules for glued-in rods and design rule proposal for implementation in European standards, Proc. CIB-W18 Meet. (2013).